Science Advances
AAAS

advances.sciencemag.org/cgi/content/full/5/1/eaau0241/DC1

Supplementary Materials for

High-throughput label-free molecular fingerprinting flow cytometry

Kotaro Hiramatsu*, Takuro Ideguchi, Yusuke Yonamine, SangWook Lee, Yizhi Luo, Kazuki Hashimoto, Takuro Ito, Misa Hase, Jee-Woong Park, Yusuke Kasai, Shinya Sakuma, Takeshi Hayakawa, Fumihito Arai, Yu Hoshino, Keisuke Goda*

*Corresponding author. Email: hiramatsu@chem.s.u-tokyo.ac.jp (K.H.); goda@chem.s.u-tokyo.ac.jp (K.G.)

Published 16 January 2019, *Sci. Adv.* **5**, eaau0241 (2019)
DOI: 10.1126/sciadv.aau0241

The PDF file includes:

Other Supplementary Material for this manuscript includes the following:

(available at advances.sciencemag.org/cgi/content/full/5/1/eaau0241/DC1)

Supplementary Materials

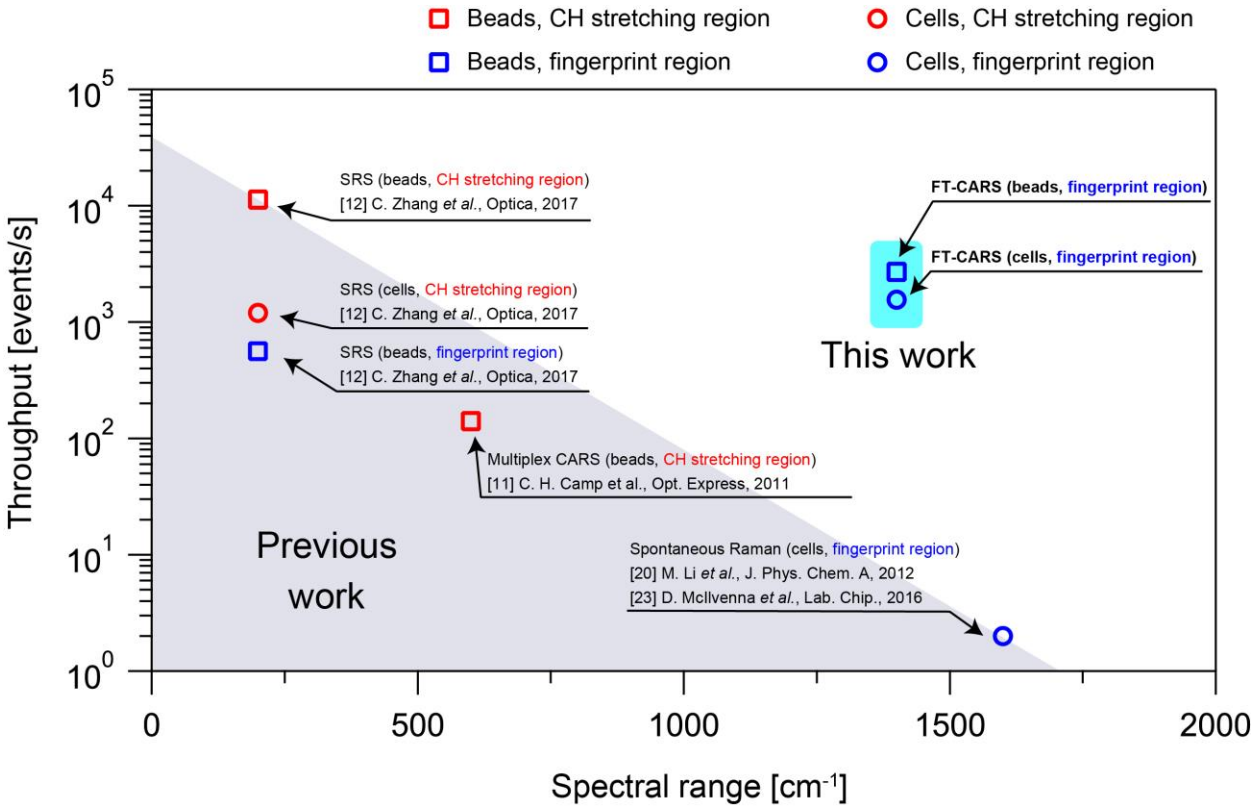

Fig. S1. Figure of merit that compares our work and previous work by others. Our work achieves both high specificity (i.e., spectral range) and high throughput and is significant for practical biological applications.

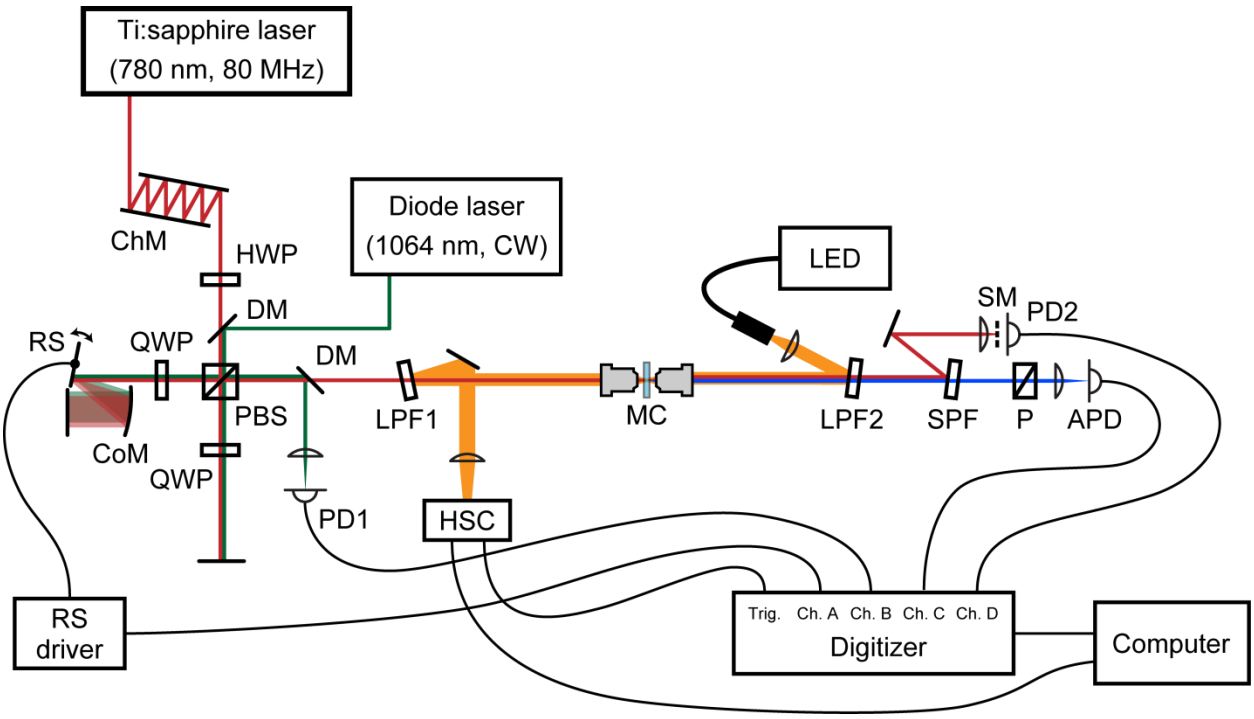

Fig. S2. Complete schematic of the FT-CARS flow cytometer. CW: continuous wave; ChM: Chirped mirror pair; HWP: Half-wave plate; DM: dichroic mirror; PBS: Polarizing beam splitter; QWP: Quarter-wave plate; RS: Resonant scanner; CoM: Concave mirror; PD1: InGaAs photodiode; HSC: High-speed camera; LPF1: Long-pass filter with a cutoff wavelength of 750 nm; MC: microfluidic chip, LPF2: Long-pass filter with a cutoff wavelength of 650 nm; SPF: Short-pass filter with a cutoff wavelength of 750 nm; P: Polarizer; APD: Avalanche photodiode; SM: Spatial mask; PD2: Si photodiode.

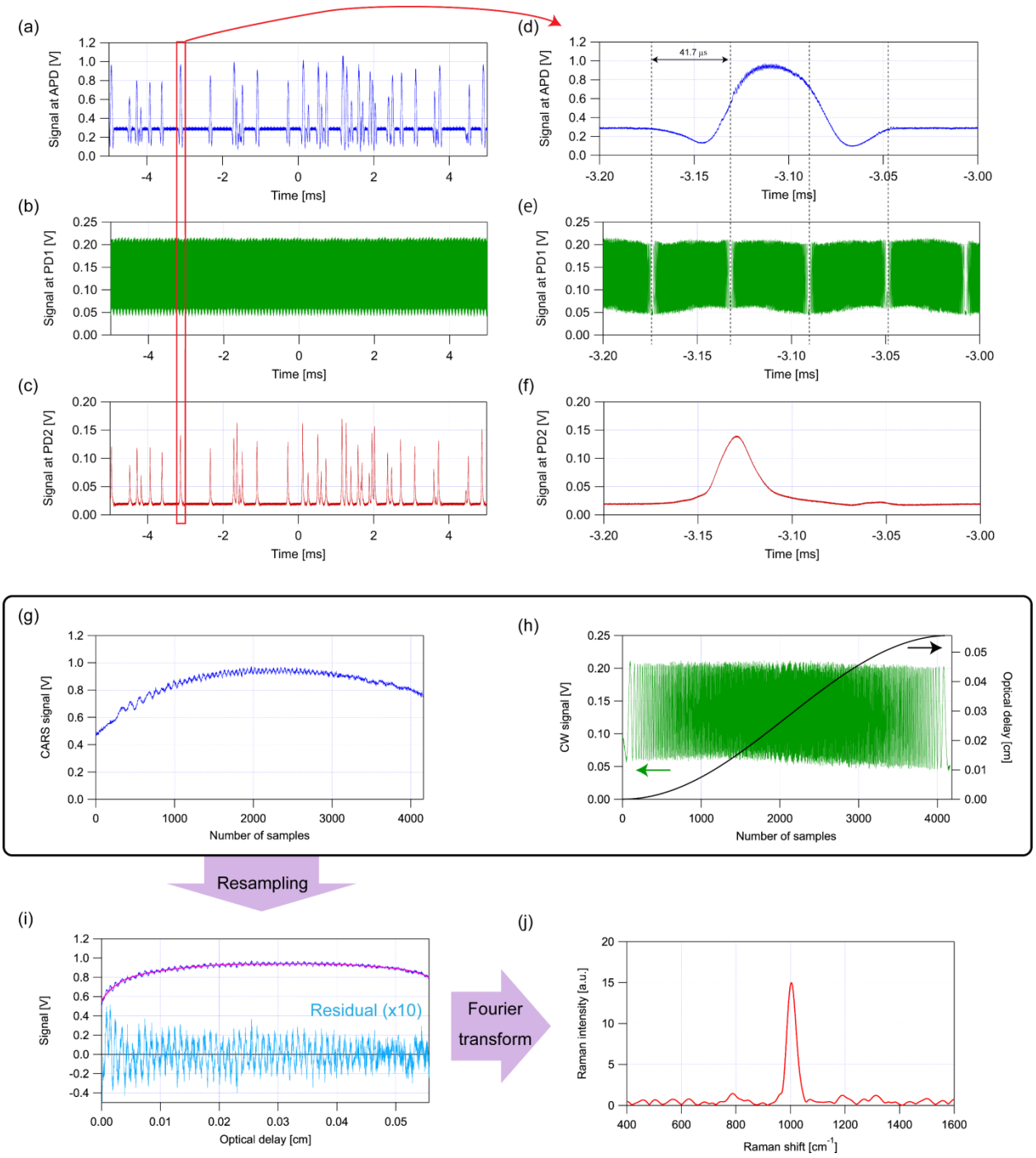

Fig. S3. Digital signal processing. (**a**) Continuous time-domain CARS interferogram of the flowing 16-µm PS beads. (**b**) Time-domain CW interferogram obtained simultaneously with the signal shown in (a). (**c**) Forward-scattering signal of the flowing 16- µm PS beads. (**d** to **f**) Enlarged views of (a to c) for a single PS bead, respectively. (**g**) Time-domain CARS interferogram of a PS bead with a single scan of the resonant scanner. (**h**) CW interferogram with a single scan of the resonant scanner (green) and optical delay produced by the pulse pair generator calculated from the CW interferogram (black). (**i**) Time-domain CARS interferogram as a function of

the optical delay (blue), slowly varying component obtained by fitting the time-domain CARS interferogram to a polynomial function (purple), and the residual of the fitting (light blue). (**j**) Single-scan FT-CARS spectrum obtained as the Fourier transform of the residual in the time-domain CARS interferogram with a Hanning window function.

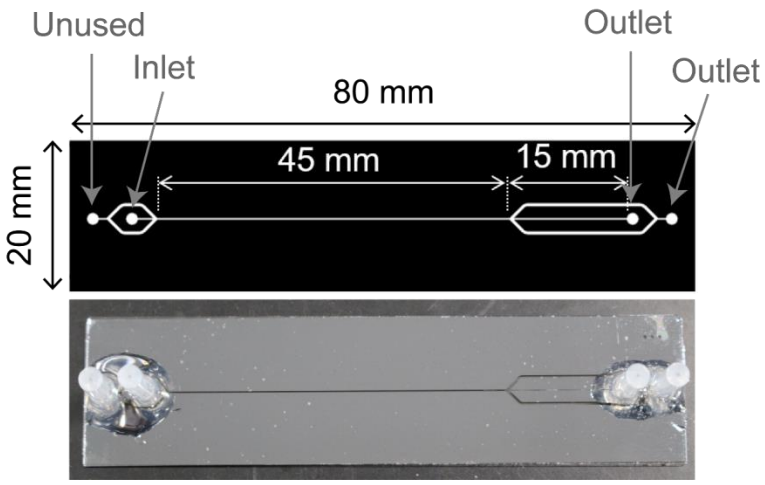

Fig. S4. Structure of the acoustofluidic-focusing microfluidic chip.

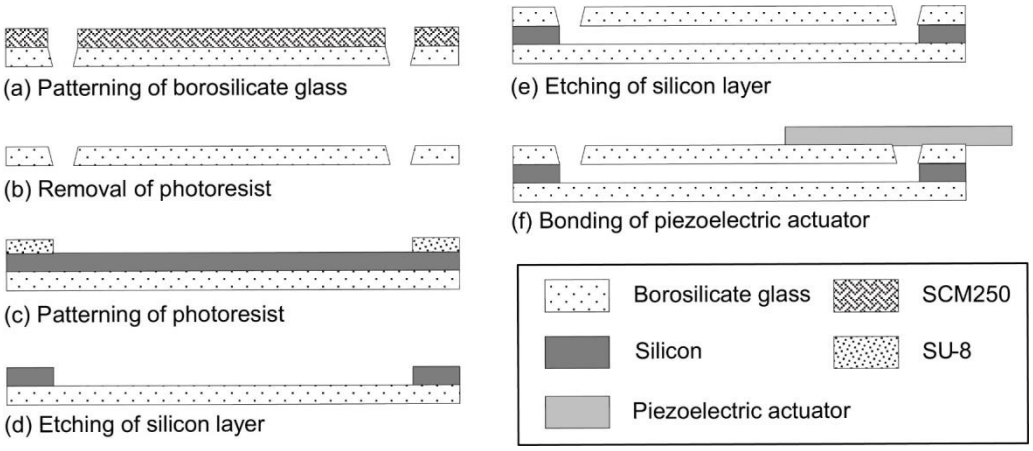

Fig. S5. Steps for fabricating the acoustofluidic-focusing microfluidic chip. (**a**) The borosilicate glass was sandblasted using an etching mask of a SCM250 (Nikko-Materials Co., Ltd., Japan) which is a negative photoresist. In this process, we obtained ports for the inlet and outlet of the microchannel. (**b**) We removed the patterned SCM250 layer. (**c**) The other borosilicate glass and silicon were bonded by using the anodic bonding technique. Then, a SU-8 (Nihon Kayaku Co., Ltd., Japan) layer was patterned on the surface of the silicon layer. (**d**) The silicon layer was etched by using the deep reactive etching technique, which allowed us to fabricate the vertical sidewalls for the microchannel. (**e**) The borosilicate glass with the ports and patterned silicon layer were bonded by using the anodic bonding technique. (**f**) A piezoelectric actuator was bonded by using a cyanoacrylate adhesive.

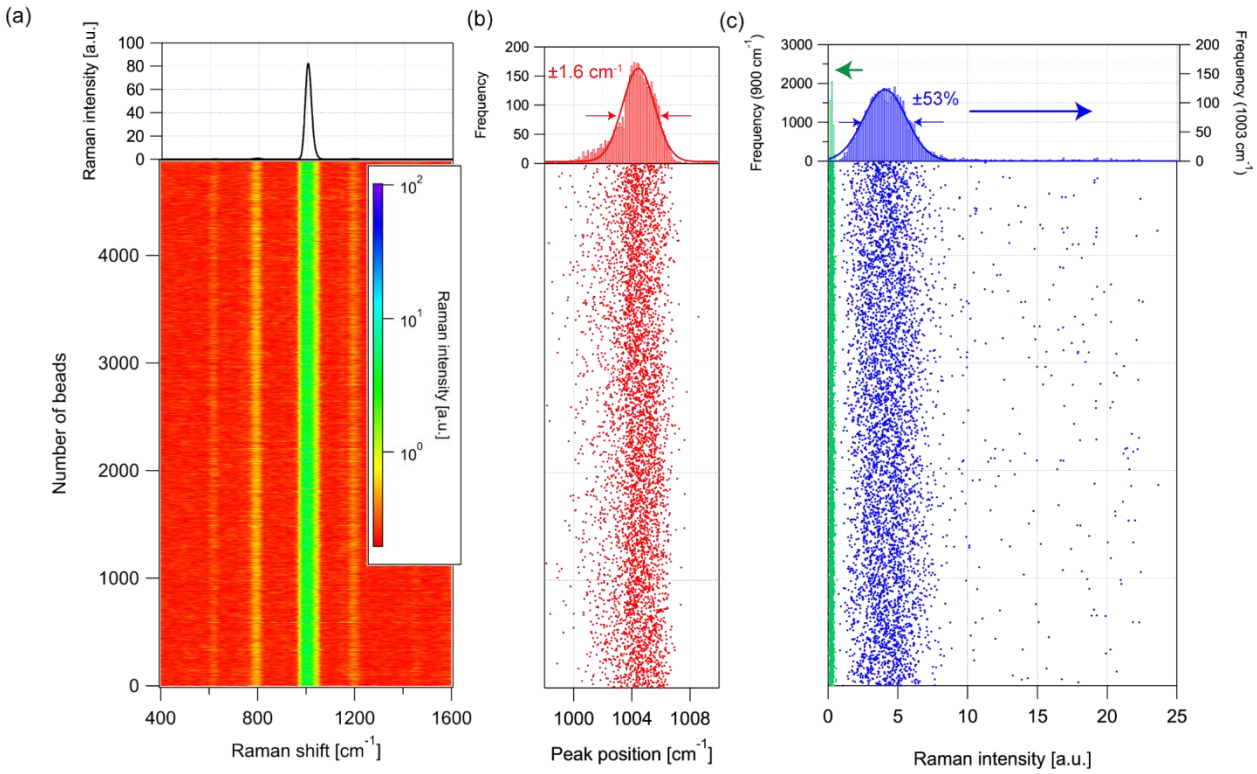

Fig. S6. Stability of the FT-CARS flow cytometer. (**a**) Bead-to-bead fluctuations of the Raman spectra of flowing PS beads (bottom) and the averaged spectrum (top) (N = 4,873). (**b**) Fluctuations of the peak position at 1,003 cm^{-1} (bottom) and its distribution with a standard deviation of 3.2 cm^{-1} (top). (**c**) Fluctuations of the peak intensity at 1,003 cm^{-1} (blue, bottom) and its distribution with a standard deviation of ±53% (blue, top). The background noise level was estimated by plotting its Raman intensity at 900 cm^{-1} (green).

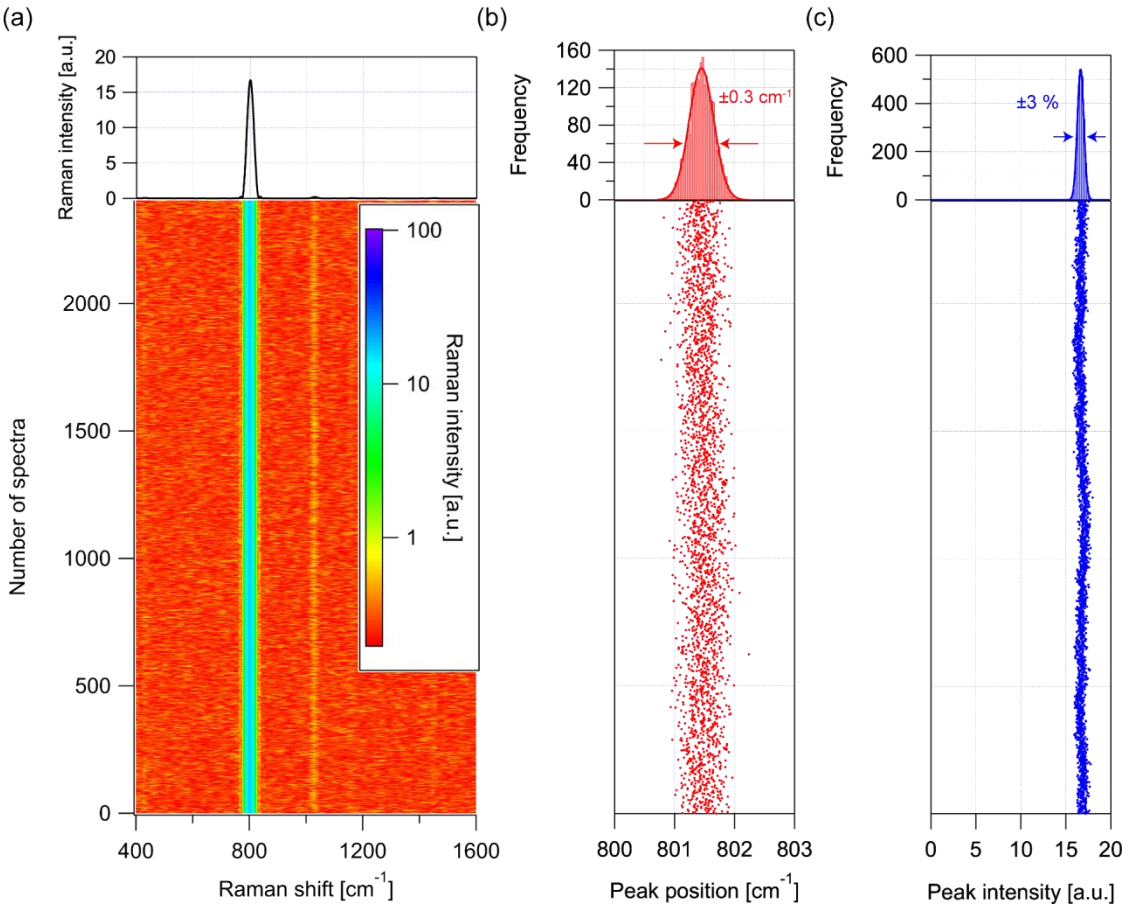

Fig. S7. Stability of the FT-CARS spectrometer. (**a**) Spectrum-to-spectrum fluctuations of the Raman spectra of cyclohexane placed on a glass slide (bottom) and the averaged spectrum (top) (N = 2,404). (**b**) Fluctuations of the peak position at 801 cm^{-1} (bottom) and its distribution with a standard deviation of 0.6 cm^{-1} (top). (**c**) Fluctuations of the peak intensity at 801 cm^{-1} (bottom) and its distribution with a standard deviation of ±3% (top).

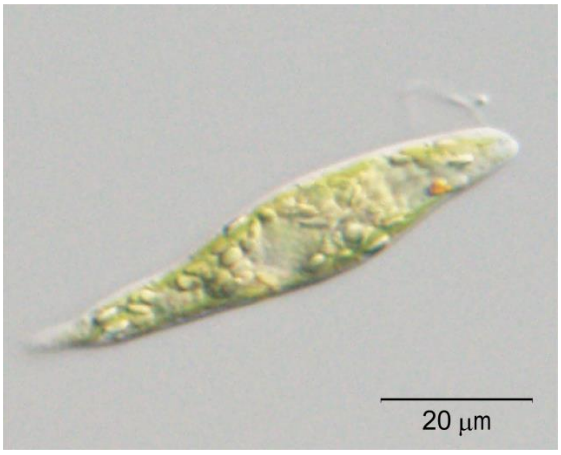

Fig. S8. Image of an *E. gracilis* cell under a conventional optical microscope.

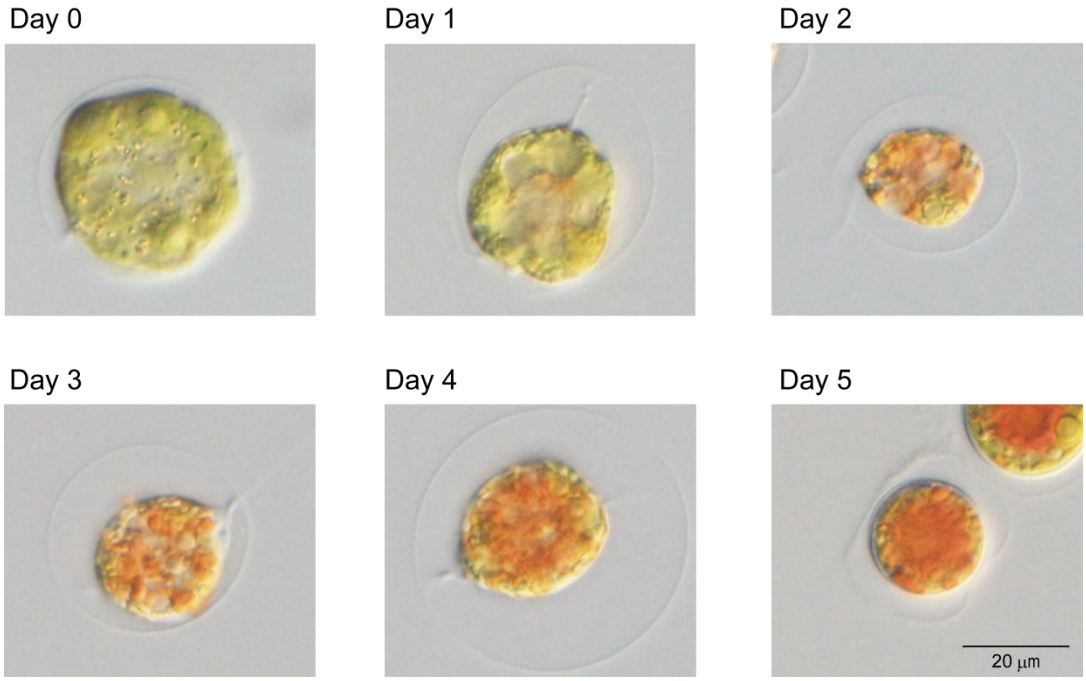

Fig. S9. Images of *H. lacustris* cells under the nitrogen deficiency stress obtained by a conventional optical microscope.

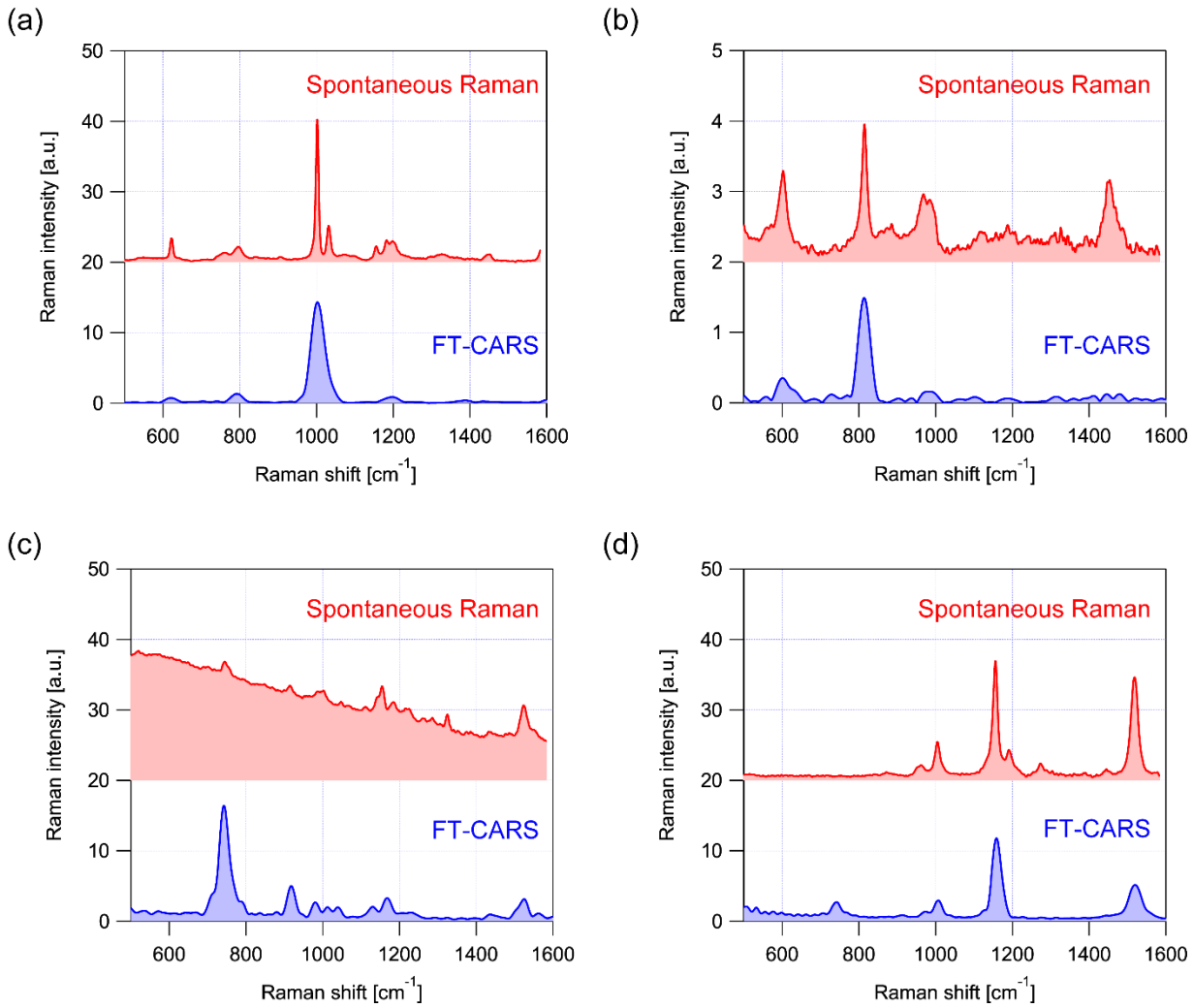

Fig. S10. Raman spectra obtained by FT-CARS and conventional spontaneous Raman spectroscopy. (**a**) PS beads. (**b**) PMMA beads. (**c**) *H. lacustris* cells on Day 0. (**d**) *H. lacustris* cells on Day 5. The spontaneous Raman spectra were obtained with a commercial Raman microscope (inVia, Renishaw) at an excitation wavelength of 785 nm. The exposure time for the spontaneous Raman spectra was 60 s. FT-CARS spectra of the PS and PMMA beads were obtained in a single scan (41.7 μs). The FT-CARS spectra of *H. lacustris* cells on Day 0 and Day 5 are given by averaging the spectra of 3,000 *H. lacustris* cells.

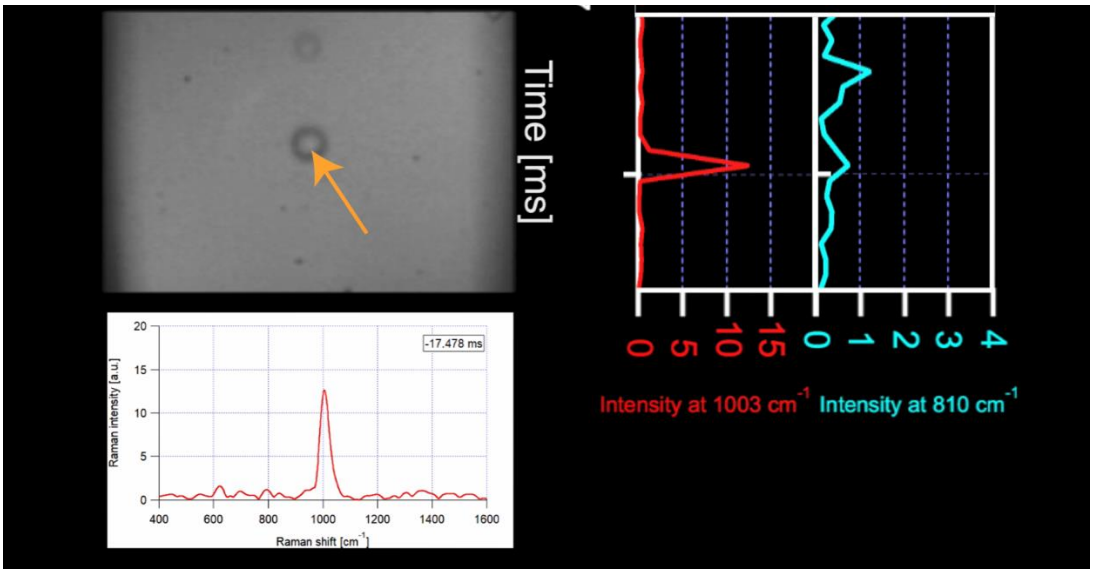

Movie S1. High-speed imaging and FT-CARS flow cytometry of fast-flowing polymer beads of multiple species. The top left panel shows the high-speed camera images of the flowing beads. The bottom panel shows the Raman spectra of the flowing beads. The right panel shows the Raman intensities at 1,000 cm^{-1} and 810 cm^{-1}.

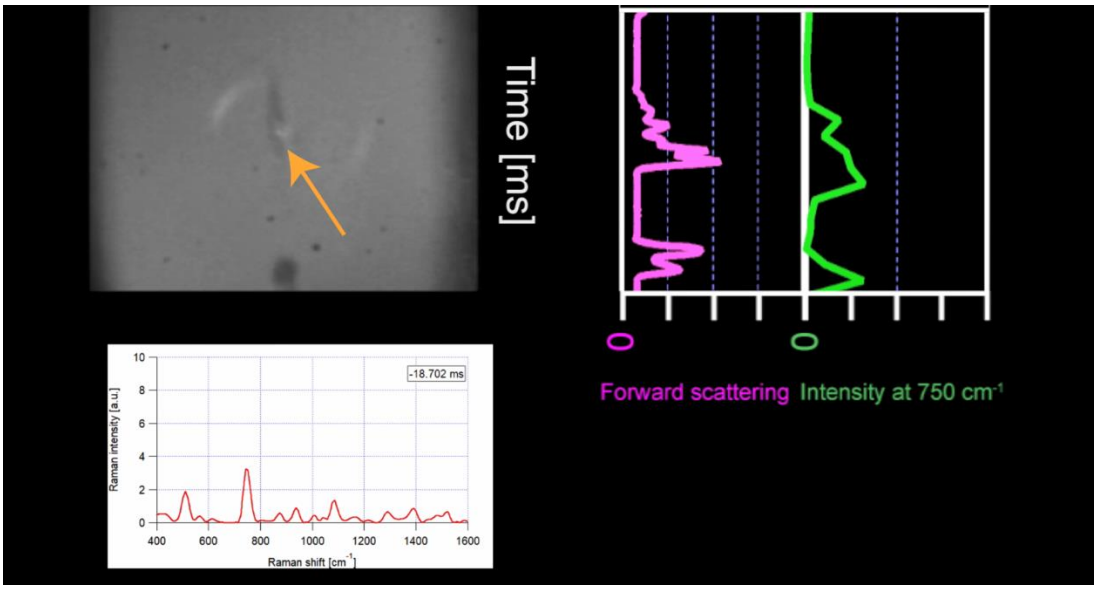

Movie S2. High-speed imaging and FT-CARS flow cytometry of fast-flowing *E. gracilis* cells. The top left panel shows the high-speed camera images of the flowing cells. The bottom panel shows the Raman spectra of the flowing cells. The right panel shows the forward-scattered light signal and Raman intensity at 750 cm^{-1}.